

TRANSVERSE EMITTANCE MEASUREMENTS OF ELECTRON BEAMS FROM THE SUPERCONDUCTING RF GUN FOR HIGH-CURRENT OPERATION AT HELMHOLTZ-ZENTRUM DRESDEN-ROSSENDORF

R. Niemczyk*, A. Arnold, A. Ryzhov, J. Teichert, R. Xiang
Helmholtz-Zentrum Dresden-Rossendorf, Dresden, Germany

Abstract

High-brightness, megahertz-rate electron sources are a crucial component of future light sources, including the Linac Coherent Light Source II High Energy project, or the high-duty-cycle upgrade of the European X-ray Free-Electron Laser. The Helmholtz-Zentrum Dresden-Rossendorf has employed a superconducting radio-frequency (SRF) gun as one of its CW electron sources for user operation at ELBE since 2010. The SRF gun is used to drive the superradiant THz source TELBE, typically at repetition rates of 50 kHz and bunch charges of 200 pC. To determine the operating envelope of the SRF gun injector, a slit-scan setup was installed in the diagnostics beamline after the SRF gun, enabling characterization of the vertical phase space. In this proceeding, we describe the slit-scan setup at the diagnostics beamline of the SRF gun. Measurements of the vertical emittance at 200 pC bunch charge and beam energies of 3.5 MeV will be presented.

CENTER FOR HIGH-POWER RADIATION SOURCES ELBE

The Helmholtz-Zentrum Dresden-Rossendorf (HZDR) operates the Center for High-Power Radiation Sources ELBE [1]. It is based on a superconducting radio-frequency (SRF) linear accelerator, which provides continuous-wave (CW) beams. Based on this accelerator, ELBE hosts multiple secondary radiation sources: the infrared free-electron laser (FEL) FELBE, the superradiant THz source TELBE, the positron source pELBE, the γ -radiation source gELBE, the neutron source nELBE, and the electron irradiation beamline eELBE. In 2024, ELBE achieved 4279 user-confirmed operation hours out of 4524 scheduled hours, corresponding to a reliability of 95 %. The facility employs two electron injectors: a thermionic injector positioned in line with the linear accelerator, and an SRF gun located in parallel. The SRF photoinjector delivers electron beams to the accelerator through a transfer dogleg.

SRF PHOTONINJECTOR

The photoinjector is based on a 3.5-cell superconducting cavity with a resonance frequency of 1.3 GHz. A normal-conducting photocathode is located in the half-cell, electrically insulated from the cavity and cooled to liquid-nitrogen temperature. Copper and magnesium have been used as photocathode materials in the past, while Cs₂Te has most recently been employed [2,3]. The Cs₂Te photocathodes had

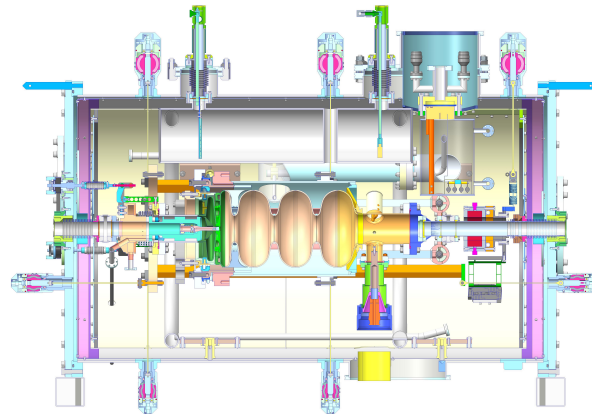


Figure 1: Cut drawing of the SRF gun-II at HZDR.

quantum efficiencies as high as 5 % inside the SRF gun and showed no significant degradation during user operation. A cross-sectional drawing of the SRF gun at HZDR is shown in Fig. 1. A DC bias voltage of -5 kV is applied to the cathode, which corresponds to 1 MV m⁻¹ of accelerating DC field. The radio-frequency field has a peak electric field strength of $E_{\text{peak}} = 17.9$ MV m⁻¹, which corresponds to a maximum electric cathode field of $E_{\text{cathode}} = 11.3$ MV m⁻¹, allowing acceleration of electrons to $E_{\text{kin}} = 3.5$ MeV. A dark current of 40 nA is present when operating the gun with this settings. The electrons are emitted from the cathode after illumination with laser pulses in the ultraviolet. When emitting 77 pC per bunch at the maximum laser repetition rate of 13 MHz, the resulting photocurrent is 1 mA. At lower repetition rate a maximal bunch charge of 300 pC can be extracted in a single bunch. More information on the SRF gun can be found in Ref. [4].

PHASE SPACE DIAGNOSTICS

For the characterization of the transverse phase space, the slit-scan technique is employed at a screen station located 2.76 m downstream of the cathode in the diagnostics beamline. The layout of the SRF gun diagnostics beamline, featuring the transfer dogleg, is depicted in Fig. 2. A 1 mm-thick mask with a 100 μ m-wide slit enables the measurement of the vertical projected emittance. The cut-out beamlets are detected on a 500 μ m-thick YAG scintillating screen located 0.75 m downstream of the slit position, and the generated light is imaged via an in-vacuum 45° mirror and an in-air 45° mirror onto a CCD camera (Basler). The imaging optics result in a screen-to-camera calibration factor

* r.niemczyk@hzdr.de

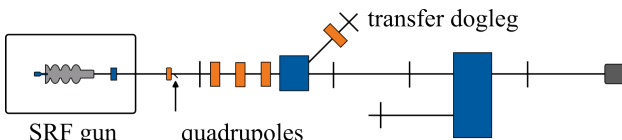


Figure 2: Schematic drawing of the SRF gun diagnostics beamline at ELBE at HZDR. The transfer dogleg allows beam transport to the linear accelerator.

of 25 $\mu\text{m}/\text{pixel}$. Further details on the diagnostics beamline are given in Ref. [5].

To prepare for user operation and beam characterization, a dedicated beam diagnostics mode was developed. While the SRF gun operates in CW mode, an acousto-optical modulator (AOM) blocks selected photocathode laser pulses, producing macropulses of laser light and thus a burst-mode electron beam pattern. This mode reduces the average beam power, thereby serving as a machine protection measure, and enables adjustment of the signal strength during beam characterization. The transverse phase space is measured by continuously moving a slit while the camera, triggered by the macro-pulse, records the integrated beamlet image. Adjusting the slit speed controls the sampling rate.

Accurate emittance calculation requires removal of noise from the beamlet images. A previously developed neural network-based image processing routine did not consistently eliminate all noise and therefore required supplementary manual noise removal [6, 7]. To address this, a traditional image processing routine was implemented. This routine applies a 3×3 median filter to the raw images, subtracts the average pixel value of a background image, and sets all pixels below $3\sigma_{\text{noise}}$ to zero, where σ_{noise} is the standard deviation of background pixel values. The horizontal projections are then used to reconstruct the transverse phase space, after which values below 1 % of the maximum phase space intensity and any unconnected satellite structures are removed.

After image processing and reconstruction of the transverse phase space the vertical emittance is calculated via

$$\epsilon_{n,y} = \beta \gamma \sqrt{\langle y^2 \rangle \langle y'^2 \rangle - \langle yy' \rangle^2}, \quad (1)$$

where β is the electron velocity in units of the speed of light, γ is the Lorentz factor, and $\langle y^2 \rangle$, $\langle y'^2 \rangle$, and $\langle yy' \rangle$ are the second-order beam moments, calculated as described in Ref. [8].

EMITTANCE MEASUREMENTS

Figure 3 shows the vertical normalized emittance measured at a bunch charge of 200 pC and an emission phase of 45°, for different solenoid magnet strengths. A bunch charge of 200 pC is standard for operation of the superradiant THz source TELBE, as the pulse energy scales with the square of the number of electrons emitting superradiantly. In routine operation, however, the emission phase is set to around 30° to achieve a more linear longitudinal phase space for

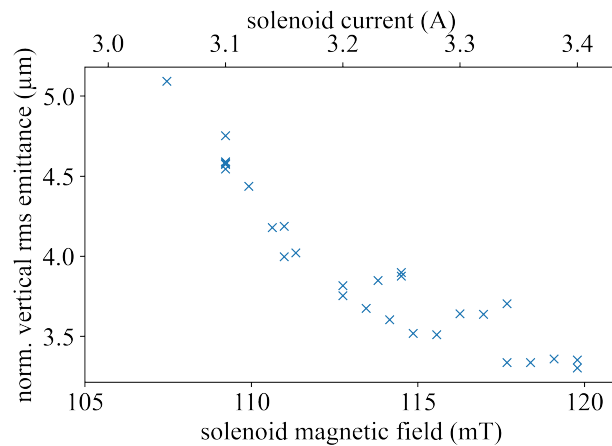


Figure 3: Vertical normalized projected emittance versus solenoid strength. The emittance values were recorded for a bunch charge of 200 pC and an emission phase of 45°.

stronger downstream compression. The solenoid current is adjusted to about 3.1 A to optimize transport through the transfer dogleg. The rms phase space ellipses and the phase space at the emittance minimum are shown in Figs. 4 and 5, respectively.

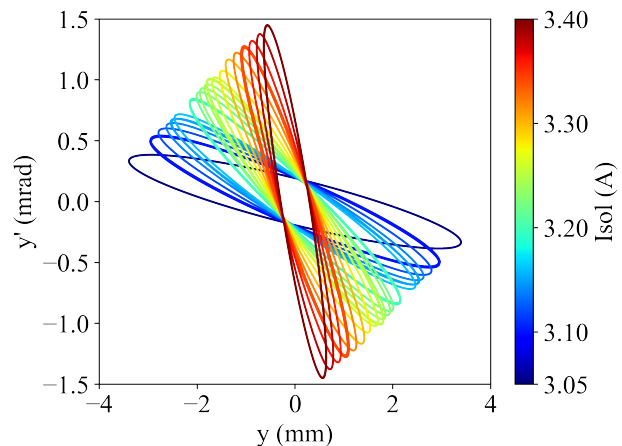


Figure 4: Transverse phase space rms ellipses in the vertical plane for different solenoid magnet strengths. The measurements were done for a bunch charge of 200 pC and an emission phase of 45 deg.

To minimize dark current contributions in the measurements, the laser repetition rate was increased to 500 kHz during the emittance measurement, compared to the 50 kHz typically used for driving the superradiant THz source. The photocathode laser pulses had a temporal Gaussian profile with a full width at half maximum (FWHM) of 5 ps. The transverse laser profile had a diameter of 4 mm on the (virtual) cathode, as shown in Fig. 6. Figure 7 shows the electron beam profile at the slit position. To compensate for quadrupole moments arising from solenoid magnet imperfections, up-right and skew quadrupole magnets were adjusted during

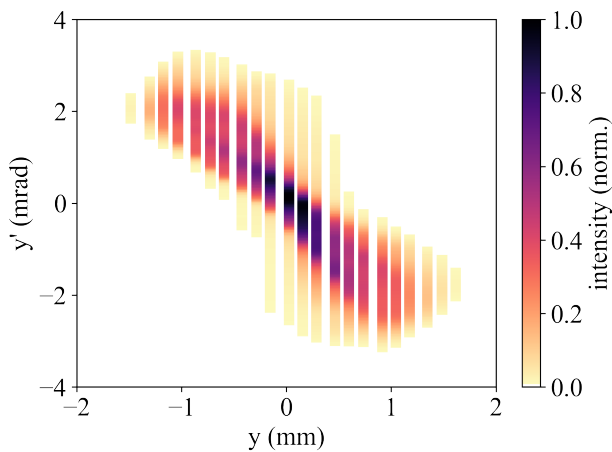


Figure 5: Transverse phase space of the electron beam in the vertical plane y . The bunch charge is 200 pC, the solenoid magnet current is 3.4 A, which corresponds to 119.8 mT of longitudinal magnetic field on axis. The vertical emittance is $3.3 \mu\text{m}$.

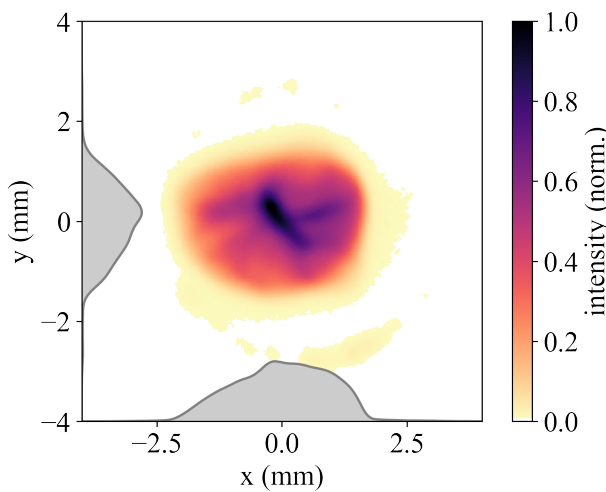


Figure 7: Electron beam distribution at the slit position. 200 pC, 45 deg, $I_{\text{sol}}=3.4 \text{ A}$. The rms beam size is $x_{\text{rms}} = 0.93 \text{ mm}$ and $y_{\text{rms}} = 0.75 \text{ mm}$.

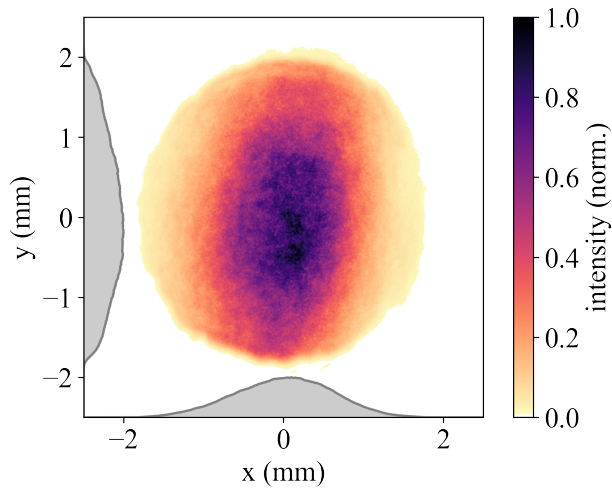


Figure 6: Transverse laser beam distribution on the virtual cathode position.

gun operation. These quadrupole settings were kept constant throughout the solenoid scan. Figure 7 also shows a photo current halo around the center at vertical positions $y = \pm 3 \text{ mm}$. We attribute this halo to a small portion of laser light that reaches the cathode due to diffraction at the edges of the beam-shaping aperture. This effect occurs even when the AOM is in the closed state, i.e., between macro-pulses, and is observed only in diagnostics mode. A lower projected emittance can be achieved using smaller laser spots and longer laser pulses. However, this is in conflict with the requirement for short electron pulses in the superradiant source and with the solenoid settings required for beam transport through the transfer dogleg. Furthermore, transport of the electron beam through the transfer dogleg causes emittance degradation. Therefore, additional optimization of the projected emittance at the SRF gun does not directly

translate into improved beam quality at the radiation source. This degradation effect becomes more pronounced at higher bunch charges. Installing the SRF gun in a straight line with the LINAC would overcome this limitation. In this configuration, the transfer dogleg could instead transport the electron beam from the thermionic injector, which would need to be relocated to the parallel beamline.

CONCLUSION AND OUTLOOK

Operation of the superradiant THz source at ELBE requires short, high-charge electron bunches. This proceedings reports the transverse rms emittance measured at the ELBE SRF gun for a bunch charge of 200 pC, the charge routinely used to drive the superradiant THz source. In combination with a newly developed image processing routine based on traditional filters, the employed slit-scan method enables characterization of the transverse phase space. Further development of the measurement software for faster data acquisition, removal of contribution by the finite slit opening to the beamlet width, as well as benchmarking of the data with particle tracking simulations, is planned.

The HZDR is planning the construction of the Dresden Advanced Light Infrastructure (DALI) [9]. DALI will be driven by an SRF gun operating at 1 mA average current and 1 nC bunch charge. As important milestones, CW operation of the SRF gun at 1 mA average current has already been demonstrated at ELBE, as well as operation of the infrared FEL. Before its installation at DALI, the next SRF gun will be experimentally benchmarked at a dedicated diagnostics beamline at HZDR, similar to the approach planned at DESY [10]. The slit-scan method is foreseen as a diagnostics tool both at this beamline and later at DALI, downstream of the SRF gun and after the LINAC modules at the full beam energy of 50 MeV. This will require a redesign of the slit-scan diagnostics to achieve higher resolution and to accommodate higher bunch charge and higher beam energy.

REFERENCES

- [1] M. Helm *et al.*, “The ELBE infrared and THz facility at Helmholtz-Zentrum Dresden-Rossendorf”, *Eur. Phys. J. Plus*, vol. 138, no. 158, Feb. 2023.
doi:[10.1140/epjp/s13360-023-03720-z](https://doi.org/10.1140/epjp/s13360-023-03720-z)
- [2] R. Xiang *et al.*, “Cs₂Te normal conducting photocathodes in the superconducting rf gun”, *Phys. Rev. ST Accel. Beams*, vol. 13, no. 4, p. 043501, Apr. 2010.
doi:[10.1103/PhysRevSTAB.13.043501](https://doi.org/10.1103/PhysRevSTAB.13.043501)
- [3] J. Teichert *et al.*, “Successful user operation of a superconducting radio-frequency photo-electron gun with Mg cathodes”, *Phys. Rev. Accel. Beams*, vol. 24, no. 3, p. 033401, Mar. 2021.
doi:[10.1103/PhysRevAccelBeams.24.033401](https://doi.org/10.1103/PhysRevAccelBeams.24.033401)
- [4] A. Arnold *et al.*, “RF Experience from 6 Years of ELBE SRF-Gun II Operation”, in *Proc. SRF’21*, East Lansing, USA, Jun.-Jul. 2021, pp. 477–481.
doi:[10.18429/JACoW-SRF2021-TUPTEV001](https://doi.org/10.18429/JACoW-SRF2021-TUPTEV001)
- [5] T. Kamps *et al.*, “Electron beam diagnostics for a superconducting radio frequency photoelectron injector”, *Rev. Sci.*
Instrum., vol. 79, no. 9, p. 093301, Sep. 2008.
doi:[10.1063/1.2964929](https://doi.org/10.1063/1.2964929)
- [6] S. Ma, “Transverse Emittance Measurements and Optimization for a Superconducting RF Photo Injector”, dissertation, Hamburg University, Hamburg, Germany, 2022.
- [7] S. Ma *et al.*, “The application of encoder-decoder neural networks in high accuracy and efficiency slit-scan emittance measurements”, *Nucl. Instrum. Methods Phys. Res. A*, vol. 1050, p. 168125, May 2023.
doi:[10.1016/j.nima.2023.168125](https://doi.org/10.1016/j.nima.2023.168125)
- [8] S.G. Anderson *et al.*, “Space-charge effects in high brightness electron beam emittance measurements”, *Phys. Rev. ST Accel. Beams*, vol. 5, no. 1, p. 014201, Jan. 2002.
doi:[10.1103/PhysRevSTAB.5.014201](https://doi.org/10.1103/PhysRevSTAB.5.014201)
- [9] DALI - Dresden Advanced Light Infrastructure, *Conceptual Design Report*, Helmholtz-Zentrum Dresden-Rossendorf, Dresden, Germany, Sep. 2023.
- [10] S. Jaster-Merz *et al.*, “Diagnostics beamline for the superconducting RF photoinjector test stand at DESY”, in *Proc. IBIC2024*, Beijing, China, Sep. 2024, pp. 207–211.
doi:[10.18429/JACoW-IBIC2024-TUP68](https://doi.org/10.18429/JACoW-IBIC2024-TUP68)